Optimization and Application of Lithium Parameters for the Reactive Force Field, ReaxFF

Sang Soo Han,[†] Adri C. T. van Duin,[‡] William A. Goddard III,[‡] and Hyuck Mo Lee*,[†]

Department of Materials Science and Engineering, Korea Advanced Institute of Science and Technology, Kusung-dong 373-1, Yusung-gu, Daejon 305-701, Korea, and Materials and Process Simulation Center, Division of Chemistry and Chemical Engineering, California Institute of Technology, Pasadena, California 91125

Received: March 21, 2005

To make a practical molecular dynamics (MD) simulation of the large-scale reactive chemical systems of Li−H and Li−C, we have optimized parameters of the reactive force field (ReaxFF) for these systems. The parameters for this force field were obtained from fitting to the results of density functional theory (DFT) calculations on the structures and energy barriers for a number of Li−H and Li−C molecules, including Li_2, LiH, Li_2H_2, H_3C-Li, H_3C-H_2C-Li, $H_2C{=}C-LiH$, $HC{\equiv}CLi$, H_6C_5-Li, and Li_2C_2, and to the equations of state and lattice parameters for condensed phases of Li. The accuracy of the developed ReaxFF was also tested by comparison to the dissociation energies of lithium−benzene sandwich compounds and the collision behavior of lithium atoms with a C_{60} buckyball.

1. Introduction

Organolithium compounds, which are increasingly important reactive intermediates, are frequently the reagents of choice for a variety of synthetic purposes because they are often more useful than other alkali metal and magnesium compounds.[1,2] However, reliable experimental data on lithium compounds is scarce. Also, because the application of high-level ab initio calculations demands high computer capacity, the development of an accurate force field (FF) for lithium is very important for carrying out molecular dynamics simulations. Generic FFs such as DREIDING[3] and UFF[4] allow predictions for broad classes of compounds, particularly when coupled with charge equilibration (QEq)[5] or other methods for predicting charges. However, in general, these force fields do not describe chemical reactivity, whereas the ReaxFF[6−8] can simulate the breaking and reforming phenomena of bonds during dynamics. Additionally, the ReaxFF is able to predict accurately not only the reactivity of bonds in the polymer systems but also the crystal and mechanical properties of the condensed phases.[6−8]

In the past decade, the semiempirical MO (molecular orbital) methods of MNDO[9] and PM3[10] for lithium compounds have been applied to obtain properties such as the heat of formation, bond length, and dipole moment. However, both methods are available to a few gas phases only; in other words, they cannot describe the condensed phases appropriately. Also, Li/MNDO is known to have some severe deficiencies (e.g., overestimation of the C−Li and H−Li interactions[9]).

In this article, we report lithium parameters for the ReaxFF. The parameters are developed by using DFT results of various organolithium compounds, and the applicability of the new parameter set is subsequently demonstrated for two cases: (i) the dissociation energies of lithium−benzene sandwich compounds, giving useful information on graphite anodic electrodes in Li ion batteries and (ii) the collision behavior of lithium atoms with a C_{60} buckyball, thereby elucidating the formation mechanism of an endohedral $Li@C_{60}$ complex. (Here, the notation $Li@C_{60}$ denotes a LiC_{60} molecule with one Li atom encapsulated inside a C_{60} cage.)

2. Computational Details

The ReaxFF framework was initially developed for hydrocarbons.[6] It was thereafter successfully employed in the study of Si/SiO_2 interfaces,[7] where the system energy is portioned into several partial energy contributions in eq 1.

$$E_{\text{system}} = E_{\text{bond}} + E_{\text{over}} + E_{\text{under}} + E_{\text{lp}} + E_{\text{val}} + E_{\text{pen}} + E_{\text{tors}} + E_{\text{conj}} + E_{\text{vdWaals}} + E_{\text{Coulomb}} \quad (1)$$

Note that the explanation for each energy term was reported in detail in a previous work.[7] Unlike the ReaxFF for hydrocarbons[6] and Si/SiO_2[7] and the total energy expression for organolithium in particular, Li−C−H systems can be considered to be a summation of electrostatic (Coulomb), bond, overcoordination, and van der Waals energies:

$$E_{\text{system}} = E_{\text{bond}} + E_{\text{over}} + E_{\text{vdWaals}} + E_{\text{Coulomb}} \quad (2)$$

Because of the relatively large ionic character of the Li−H and Li−C bonds,[11,12] angle bending and torsion terms in the total energy are not included because they were all set equal to zero. The Coulomb interactions in our ReaxFF were calculated between all atom pairs with the atomic charges. They are determined for each configuration using the electron equilibration method (EEM).[13] We optimized the EEM parameters (electronegativity χ, chemical hardness η, and shielding radius r) to reproduce the charge distribution of numerous clusters, shown in Figure 1, involving Li, C, and H obtained from DFT calculations using the JAGUAR code[14] with the B3LYP (Becke three-parameters plus Lee−Yang−Parr) functional and a 6-31G** basis set. The EEM parameters for C and H were determined in a previous study.[6]

* To whom correspondence should be addressed. E-mail: hmlee@kaist.ac.kr.
[†] Korea Advanced Institute of Science and Technology.
[‡] California Institute of Technology.

10.1021/jp051450m CCC: $30.25
Published on Web 05/03/2005

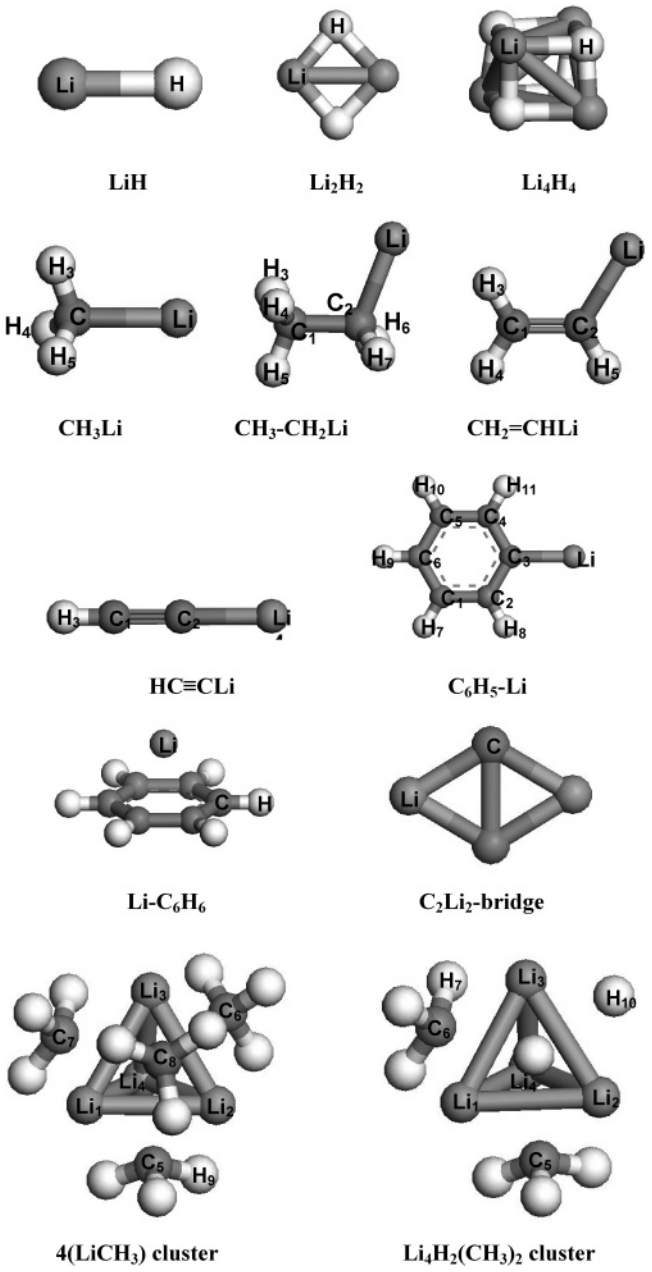

Figure 1. Molecules used to develop the ReaxFF parameters of Li in this study.

For Li crystals, we fitted various phases of Li, including fcc (12), hcp (12), bcc (8), sc (6), and diamond (4), which effectively allowed us to vary the coordination number of Li. In DFT calculations on our periodic systems, we employed the generalized gradient approximation of the Perdew−Burke−Ernzerholf functional[15] for the exchange-correlation potential and ultrasoft pseudopotentials to replace the core electrons, implemented in the CASTEP code.[16] We set a kinetic energy cutoff of 180.0 eV for Li and used the Monkhorst−Pack scheme[17] to generate the k-space grid. We also found that a k-point sampling of 666 was sufficient for convergence.

3. Results and Discussion

3.1. Bond Dissociation. Structures depicted in Figure 1 are determined through full geometry optimizations to find ground-state structures. Dissociation profiles are then constructed through total energy calculations at the modified geometries only by changing the bond length from its equilibrium value, which is shown in Figure 2.

To optimize the ReaxFF bond energies, we first carried out DFT calculations for the dissociation of single bonds of Li−Li and Li−H. Parts a and b of Figure 2 provide comparisons of the DFT and ReaxFF results for single-bond dissociations of Li−Li and Li−H in Li_2 and LiH systems. We used DFT methods for the singlet state from the equilibrium distance up to the point where it was comparable to the dissociation limit (to the lowest of either the singlet or triplet full bond dissociation energies). In Figure 2a, the equilibrium bond distance and bond dissociation energy of a Li_2 molecule, calculated by DFT, are 2.73 Å and 20.24 kcal/mol, respectively. Fuentealba and Reyes[18] reported that the theoretical (B3PW91 level and 6-311G** basis set) and experimental dissociation energies for Li_2 are 18.54 and 24.42 kcal/mol, respectively, thus verifying that our DFT calculation result is reliable. Using the ReaxFF, the bond distance and bond dissociation energy are 2.72 Å and 33.28 kcal/mol, respectively. According to MNDO and PM3 calculations, the bond distances of Li_2 are 2.48[9] and 2.05 Å,[10] respectively, which implies that the ReaxFF estimates the bond distance more accurately than the MNDO and PM3 methods. However, it overestimates the dissociation energy of the Li_2 molecule. When the parameters of Li for the ReaxFF were fitted in the present study, gas phases as well as crystal information as reference data calculated by DFT were used. Because the bond energy of $Li-Li^+$ is 33.7 kcal/mol[19] and the cohesive energy of a Li crystal with bcc structure is 37.7 kcal/mol,[20] the bond character between two Li atoms in the solid Li is $Li-Li^+$, not Li−Li.[19] The ReaxFF cannot provide an accurate description of the ionic state. Therefore, when the ReaxFF parameters of Li were optimized, the Li−Li single-bond dissociation energy in a Li_2 molecule was overestimated to describe accurately information for the condensed phases of Li, causing a certain degree of inaccuracy for Li_2 molecules.

For a LiH molecule (Figure 2b), the DFT shows an equilibrium bond distance of 1.62 Å and a bond dissociation energy of 58.95 kcal/mol, and the ReaxFF yields estimates of 1.58 Å and 59.66 kcal/mol, which are in good agreement with the DFT results. The reliability of our results for LiH is verified by comparison with those of Fuentealba and Reyes.[18] They reported that the theoretical and experimental dissociation energies for LiH are 69.97 and 58.06 kcal/mol, respectively. The MNDO and PM3 methods predict the bond distance to be 1.54[9] and 1.38 Å,[10] respectively, thus demonstrating that the ReaxFF describes the bond distance of a LiH molecule more accurately than these approaches.

Parameters for the Li−C single bond were also determined by DFT calculations on CH_3Li, CH_3-CH_2Li, $CH_2=CHLi$, HC≡CLi, and C_6H_5Li molecules. Parts c−g of Figure 2 show curves for single-bond dissociations of Li−C for the CH_3Li, CH_3-CH_2Li, $CH_2=CHLi$, HC≡CLi, and C_6H_5Li systems. The optimized conformational information of each molecule is provided in Table 1. The information in Table 1 shows that the ReaxFF is superior to the MNDO and PM3 methods in terms of a conformational prediction of the above molecules. For a methyllithium (CH_3Li) molecule (Figure 2c and Table 1), the DFT results show that the equilibrium Li−C bond distance is 1.98 Å and the bond dissociation energy is 55.12 kcal/mol. According to the ReaxFF method, the Li−C bond distance is 2.09 Å, and the bond dissociation energy is 52.71 kcal/mol, which is about 3 kcal/mol lower than that obtained through the DFT calculation. For the CH_3-CH_2Li molecule (Figure 2d and Table 1), the DFT calculation indicates that the equilibrium

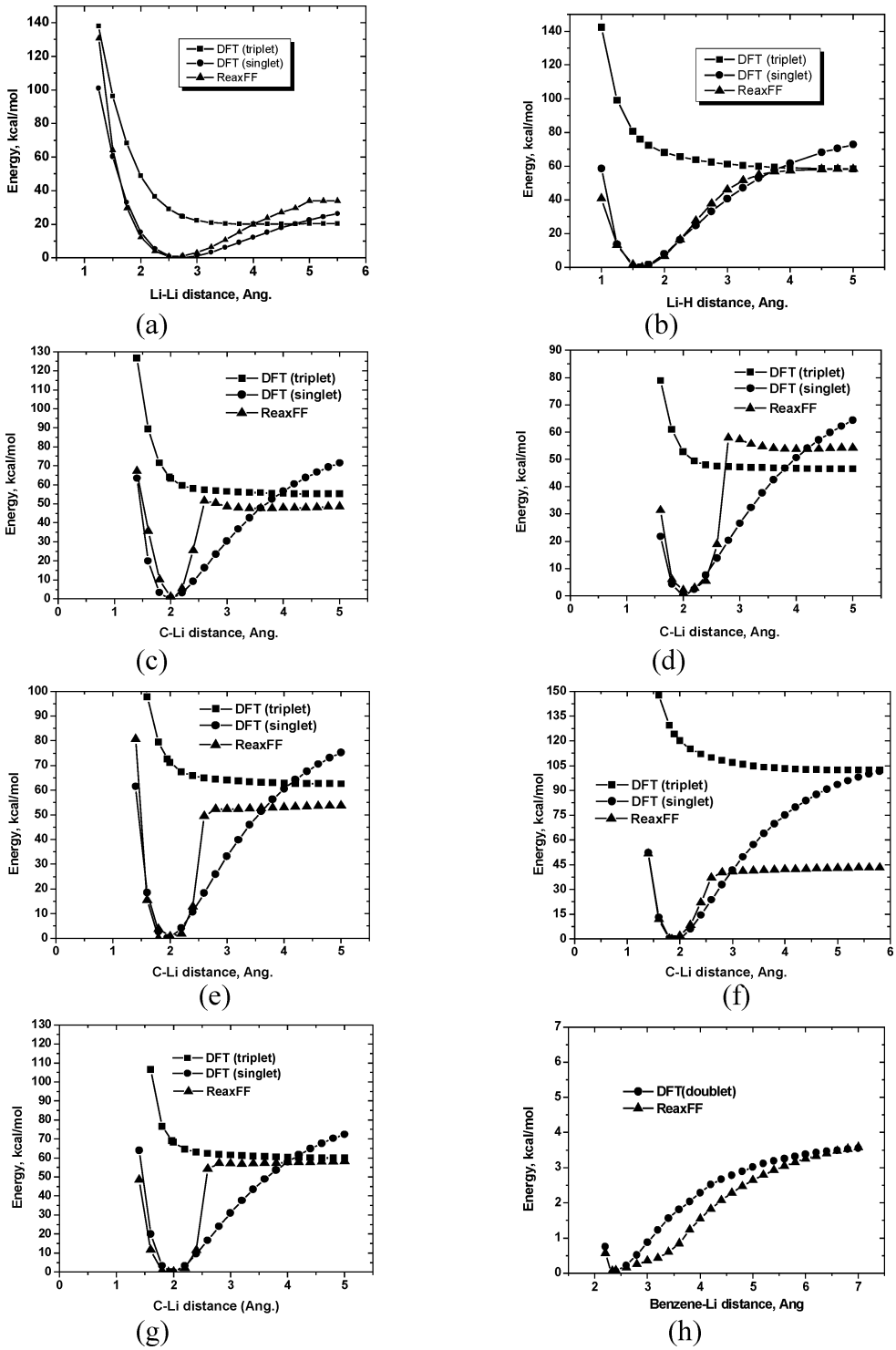

Figure 2. DFT and ReaxFF data for bond dissociations of various Li−C−H systems: (a) the Li−Li single bond in Li_2, (b) the Li−H bond in LiH, (c) the Li−C bond in CH_3Li, (d) the Li−C bond in CH_3-CH_2Li, (e) the Li−C bond in $CH_2{=}CHLi$, (f) the Li−C bond in $HC{\equiv}CLi$, (g) the Li−C bond in C_6H_5Li, and (h) the van der Waals interaction of a Li atom on a benzene ring.

Li−C bond distance is 2.01 Å and the bond dissociation energy is 46.51 kcal/mol. The ReaxFF gives an equilibrium Li−C bond distance of 2.01 Å, which is very similar to the DFT value, and a bond dissociation energy of 55.15 kcal/mol, which is higher than the DFT value. One C−C bond in the CH_3-CH_2Li molecule is a single bond, and the Li−C bonding character may be affected by the C−C bond order near the Li−C bond. To investigate this, we additionally considered $CH_2{=}CHLi$ and $HC{\equiv}CLi$ molecules. The bond order between two carbon atoms in $CH_2{=}CHLi$ is 2 (a double bond—one σ bond and one π bond), and that in $HC{\equiv}CLi$ is 3 (a triple bond—one σ bond and two π bonds). As shown in Figure 2e and Table 1, the DFT calculation reveals that the equilibrium distance of the Li−C bond in the $CH_2{=}CHLi$ molecule (C−C bond order of 2) is 1.95 Å, which is shorter than that (2.01 Å) of the CH_3-CH_2Li molecule. The dissociation energy of the Li−C bond is 62.53 kcal/mol, which is larger than that (46.51 kcal/mol) of CH_3-CH_2Li. The ReaxFF indicates that the bond distance of Li−C is 1.77 Å, which is 0.18 Å shorter than the DFT result, and the dissociation energy of the bond is estimated to be 58.57

TABLE 1: Optimized Geometries of Various Organolithium Molecules

parameter[a]	DFT	ReaxFF	PM3[b]	MNDO[c]	parameter[a]	DFT	ReaxFF	PM3[b]	MNDO[c]
					CH_3Li				
$r(CLi)$	1.978	2.099	2.525	1.821	$\angle(H_3CLi)$	112.47	110.87	91.74	111.92
$r(CH_3)$	1.100	1.124	1.063	1.117	$\angle(H_3CH_4)$	106.31	108.03	119.91	106.92
					CH_3-CH_2Li				
$r(C_2Li)$	2.005	2.029	2.868	1.829	$\angle(H_6C_2Li)$	108.28	113.53	95.01	116.05
$r(C_1C_2)$	1.542	1.523	1.430	1.528	$\angle(C_1C_2Li)$	117.46	95.90	95.35	97.04
$r(C_2H_6)$	1.103	1.118	1.075	1.114					
					$CH_2=CHLi$				
$r(C_2Li)$	1.954	1.797	2.862	1.784	$r(C_2H_5)$	1.100	1.162	1.097	1.094
$r(C_1C_2)$	1.349	1.274	1.319	1.352	$\angle(H_5C_2Li)$	127.49	136.84	125.45	144.70
$r(C_1H_3)$	1.095	1.121	1.090	1.112	$\angle(C_1C_2Li)$	120.17	101.89	118.56	119.59
					$HC\equiv CLi$				
$r(C_2Li)$	1.897	1.849	2.868	1.744	$\angle(C_1C_2Li)$	180.00	180.00	180.00	180.00
$r(C_1C_2)$	1.230	1.216	1.216	1.213	$\angle(H_2C_1C_2)$	180.00	180.00	180.00	180.00
$r(C_1H_3)$	1.068	1.101	1.057	1.052					
					C_6H_5Li				
$r(C_3Li)$	1.973	1.920	2.857	1.797	$\angle(C_2C_3C_4)$	114.60	122.20	116.34	117.85
$r(C_2C_3)$	1.416	1.388	1.393	1.413	$\angle(C_2C_3Li)$	122.68	118.90	121.86	121.10
$r(C_2H_8)$	1.092	1.112	1.095	1.097	$\angle(C_3C_4H_{11})$	119.73	121.63	118.35	120.02

[a] See Figure 1. [b] Reference 10. [c] Reference 9.

kcal/mol, which is quite reasonable. Results for HC≡CLi (C−C bond order of 3) are presented in Figure 2f and Table 1. According to the DFT calculation, the bond distance and bond dissociation energy of Li−C in HC≡CLi are 1.90 Å and 102.79 kcal/mol, respectively. The ReaxFF provides a good description of the conformation of the molecule. However, there is a large difference between the dissociation energy of the Li−C bond predicted by the ReaxFF and DFT, revealing the most serious problem in the present ReaxFF for Li. We also considered phenyl-lithium (C_6H_5Li), which has a C−C bond order of 1.5. In Figure 2g and Table 1, the ReaxFF correctly describes the dissociation energy of the Li−C bond and conformation information of phenyl-lithium. From the dissociation curves (parts c−g of Figure 2) of Li−C bonds in various organolithium molecules expressed thus far, we also found that the dissociation curves estimated by the ReaxFF method have a U shape. For instance, in the case of phenyl-lithium (Figure 2g), the dissociation curve appears to be U-shaped up to about 2.8 Å, after which the energy remains constant, thus indicating that a Li−C bond in phenyl-lithium is broken at about 2.8 Å. From the DFT calculation, Li−C bond breaking occurs from 2.6 to 2.8 Å, which is consistent with the ReaxFF result. From the results thus far, we can determine that the Li−C bonding character in an organolithium system is affected by a C−C bond near the Li−C bond. In other words, the higher the bond order of a C−C bond in organolithium molecules, the shorter the bond distance of the Li−C bond near the C−C bond and the higher the bond energy of the Li−C bond.

3.2. van der Waals Interaction. The van der Waals interaction in the ReaxFF is used with a distance-corrected Morse potential including a shielded interaction.[6,7] Parameters for a Li atom related to the van der Waals interaction are the van der Waals radius (r_{vdW}), van der Waals dissociation energy (ϵ), van der Waals parameter (α), and van der Waals shielding (γ_{vdW}). To determine these parameters, we considered the interaction of a Li atom on a benzene ring (Figure 1). Figure 2h indicates the change in the van der Waals energy of a Li atom on a benzene ring with respect to the distance from the Li atom to the center of the ring. The ReaxFF can quite accurately explain the van der Waals interaction of a Li atom on a benzene ring. The DFT calculation indicates that 2.33 Å is the distance between the Li atom and the center of the benzene ring in the optimized structure, whereas the ReaxFF yields a very similar predication of 2.32 Å. The DFT calculation in this study was performed with the B3LYP functional. The DFT method may not provide a good explanation of the van der Waals interaction.[21] To assess the disadvantage of the B3LYP, which may occur in the van der Waals interaction of the Li atom upon the benzene ring, we also used the X3LYP functional[22] for the system. The X3LYP leads to an accurate description of van der Waals.[23] For example, previously reported high-quality ab initio calculations [MP4/6-311G(d,p)//MP2/6-311G(d,p)] indicated that a Li cation binds six H_2 molecules at zero Kelvin with enthalpies for adding successive H_2 of −5.39, −4.30, −4.07, −3.65, −1.87, and −2.30 kcal/mol;[23] these values agree well with the X3LYP results of −5.12, −4.47, −3.9, −3.63, −1.55, and −1.52 kcal/mol for the same system.[24] The X3LYP result for the system considered in this study is very similar to the B3LYP result. Therefore, we confirmed that the B3LYP functional can appropriately describe the van der Waals interaction of a Li atom on a benzene ring.

3.3. Charge Distribution. As already mentioned, in the case of lithium, the ionic bond character is larger than the covalent bond character.[11,12] Hence, we did not consider valence angle terms such as C−Li−C and Li−C−Li. Instead, we focused on atomic charge terms such as EEM electronegativity (χ), EEM hardness (η), and EEM shielding (γ) in optimizing the ReaxFF parameters. Shown in Figure 1 are all of the molecules that we considered to determine the three atomic charge terms of Li. Charge distributions in the ReaxFF are calculated using the EEM method.[6,7] The EEM parameters were optimized against the Mulliken charge distribution obtained from DFT calculations. The ReaxFF results for the atomic charges of all molecules depicted in Figure 1 are summarized in Table 2. For a Li_2H_2 molecule with a bridged structure, the DFT/Mulliken partial charges for Li and H atoms are 0.1670 and −0.1670, respectively, whereas the ReaxFF calculates partial charges of 0.1696 and −0.1696 for the Li and H atoms, respectively. In the case of methyl-lithium (CH_3Li), the ReaxFF assigns partial charges to C, H, and Li of −0.4649, 0.0771, and 0.2318, respectively, compared to DFT/Mulliken values of −0.5507, 0.0715, and 0.3362, respectively. Overall, the ReaxFF gives a good prediction of the partial atomic charges of various organolithium molecules except for Li on a benzene ring.

TABLE 2: Optimized Charge Distributions of Various Organolithium Molecules

molecule[a]	DFT	ReaxFF	molecule[a]	DFT	ReaxFF
		LiH			
Li	0.3853	0.1398	H	−0.3853	−0.1398
		Li_2H_2			
Li	0.1670	0.1696	H	−0.1670	−0.1696
		Li_4H_4			
Li	0.1993	0.2001	H	−0.1993	−0.2001
		CH_3Li			
C	−0.5507	−0.4649	H_3	0.0715	0.0771
Li	0.3362	0.2318			
		CH_3-CH_2Li			
C_1	−0.2895	−0.2888	H_5	0.0685	0.0904
C_2	−0.3951	−0.3365	H_6	0.0631	0.0795
H_3	0.0776	0.0624	H_7	0.0631	0.0795
H_4	0.0776	0.0624	Li	0.3347	0.2511
		$CH_2=CHLi$			
C_1	−0.2252	−0.2143	H_4	0.0592	0.0933
C_2	−0.2543	−0.3256	H_5	0.0355	0.0972
H_3	0.0489	0.0487	Li	0.3359	0.3006
		HC≡CLi			
C_1	−0.2720	−0.1131	H_3	0.0938	0.0881
C_2	−0.2033	−0.2651	Li	0.3815	0.2901
		C_6H_5Li			
C_2	−0.1347	−0.0894	H_8	0.0376	0.0625
C_3	−0.1233	−0.1798	Li	0.3767	0.2672
		$Li-C_6H_6$			
Li	−0.2472	0.2966	H	0.1233	0.0795
C	−0.0821	−0.1290			
		C_2Li_2 Bridge			
Li	0.1695	0.2404	C	−0.1695	−0.2404
		4($LiCH_3$) Cluster			
Li_1	0.2876	0.3900	C_6	−0.6082	−0.5211
Li_2	0.2849	0.3912	C_7	−0.6081	−0.5213
Li_3	0.2857	0.3908	C_8	−0.6080	−0.5212
Li_4	0.2850	0.3904	H_9	0.1074	0.0435
C_5	−0.6078	−0.5213			
		$Li_4H_2(CH_3)_2$ Cluster			
Li_1	0.3814	0.2334	C_5	−0.6155	−0.5329
Li_2	0.1034	0.3221	C_6	−0.6165	−0.5329
Li_3	0.1047	0.3220	H_7	0.1074	0.0588
Li_4	0.3719	0.2334	H_{10}	−0.1905	−0.1894

[a] See Figure 1.

3.4. Crystal. Simulations of the condensed-phase Li can be a key application for the ReaxFF. The ability of the ReaxFF potential to predict condensed-phase stabilities was tested against a variety of crystal structures for Li. For the five lithium crystal structures of fcc, hcp, bcc, sc, and diamond, the DFT energies were obtained for a broad range of compression and expansion and then compared against the ReaxFF in Figure 3. Also, for each phase of Li, the lattice parameters and phase stabilities were compared against DFT data, which is expressed in Tables 3 and 4. The ReaxFF correctly describes equations of state of fcc, hcp, bcc, and sc; however, for the diamond-structured Li crystal, the ReaxFF overestimates the lattice parameter of the diamond structure. Except for the diamond structure case, the ReaxFF predicts the lattice parameters very well and also accurately estimates the phase stability for the five Li crystals. According to several experimental[25] and theoretical[26,27] studies, Li is in a close-packed structure (fcc or hcp) at low pressure and temperature and is in a bcc structure at room temperature, which supports our DFT results for Li crystals. Figure 3a and Table 4 reveal that the fcc structure for Li is most stable at zero Kelvin. Moreover, we also discovered that equations of state for fcc, hcp, and bcc structures of Li almost overlapped with volume change. For this reason, the crystal structure of Li may be transformed relatively easily by pressure and/or temperature. Young and Ross[26] predicted two transitions below 1 Mbar on the 0 K isotherm: hcp−fcc at about 4 kbar and fcc−bcc at about 86 kbar. Also, we compared the cohesive energy of bcc Li, calculated by DFT and ReaxFF. The cohesive energy by the DFT calculation is −43.00 kcal/mol, whereas the ReaxFF

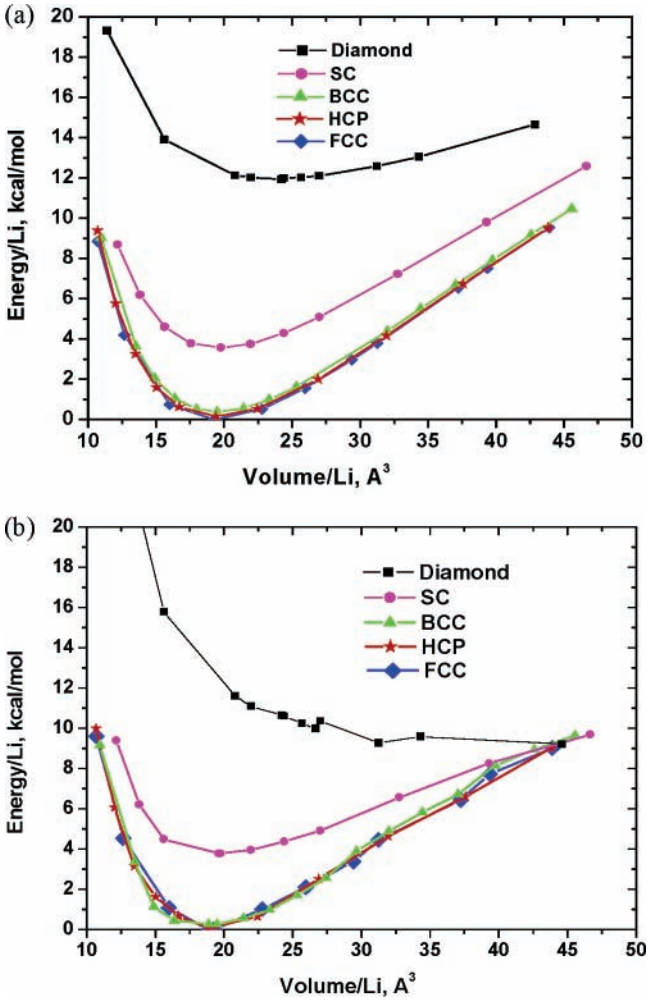

Figure 3. Equations of state (compression and tension) for five crystal structures (HCP, FCC, BCC, SC, and diamond) of lithium calculated using (a) DFT and (b) ReaxFF methods.

TABLE 3: Lattice Parameters for Five Structures (HCP, FCC, BCC, SC, and Diamond) of Lithium Calculated by DFT and ReaxFF

	lattice parameter (Å)	
crystal structure	DFT	ReaxFF
HCP	a: 3.048, c: 4.819	a: 3.052, c: 4.827
FCC	4.257	4.291
BCC	3.390	3.363
simple cubic (SC)	2.704	2.642
diamond	5.785	7.179

TABLE 4: Phase Stabilities (kcal/mol of Li) for Five Lithium Strucutres Relative to BCC-Structured Li

crystal structure	ΔE_{DFT}	ΔE_{ReaxFF}
HCP	−0.2325	−0.2483
FCC	−0.3724	−0.3392
SC	3.1997	2.7238
diamond	11.5681	11.0107

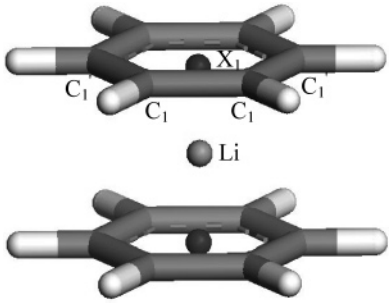

Figure 4. Structure and labels for the optimized $Li\cdot(C_6H_6)_2$ complex, predicted by ReaxFF.

TABLE 5: Optimized Geometries of the $Li\cdot(C_6H_6)_2$ Complex

parameter	quantum calculation[33]	ReaxFF
$r(C_1C_1)$	1.393[b] (1.391)[c]	1.406
$r(C_1C_1')$	1.422 (1.422)	1.406
$r(C_1H_1)$	1.088 (1.087)	1.054
$r(C_1H_1')$	1.085 (1.084)	1.054
$r(LiX_1)$[a]	1.769 (1.872)	2.140
$\angle(C_1C_1'C_1)$	118.3 (118.6)	120.0
$\angle(C_1C_1'C_1)$	120.7 (120.7)	120.0
$d(C_1C_1'C_1C_1)$	6.1 (4.0)	0.0

[a] X_1 refers to the center of the benzene ring. Bond and dihedral angles are in degrees, and bond lengths are in angstroms. (See Figure 11 for definitions of labels.) [b] MP2(FC)/6-31G(d) results. [c] B3LYP/6-31G(d) results in parentheses.

underestimates the value as −34.48 kcal/mol, which is similar to the experimental value (−37.70 kcal/mol)[20] extrapolated to zero Kelvin.

3.5. Applications. *3.5.1. Dissociation Energy of Lithium−Benzene Sandwich Compounds.* There is considerable interest in the intercalation of Li into graphite because of the widespread use of graphite/carbon anodes in lithium ion batteries.[28,29] To gain a fundamental understanding of Li−intercalated graphite, it is necessary to understand the interactions between lithium and π electrons of aromatic carbon. In this study, the structures and dissociation energies of $Li_n\cdot(C_6H_6)_{n+1}$ sandwich complexes ($n = 1-6$) have been investigated using the ReaxFF developed in this work and compared with the quantum chemical data.[30]

Optimized geometries for a $Li\cdot(C_6H_6)_2$ system, predicted by quantum chemical methods[30] such as MP2, B3LYP, and ReaxFF, are presented in Figure 4 and Table 5, where the quantum calculations are for a D_{2h} structure. According to quantum calculations,[30] the $Li\cdot(C_6H_6)_2$ complex exhibits a Jahn−Teller distortion in which both benzene rings distort from their planar geometry, "folding" on an axis between the C_1' carbon atoms with the fold away from the lithium atom. In contrast, this behavior is not found by the ReaxFF, which indicates that the benzene rings remain in a planar structure. For example, $d(C_1C_1'C_1C_1)$ is 6.1 by the MP2 method, whereas it is 0.0 by the ReaxFF. We also found that the ReaxFF overestimates the distance between the Li atom and the center of the benzene ring compared to the quantum calculation.

Table 6 shows the dissociation energies of the $Li_n\cdot(C_6H_6)_{n+1}$ sandwich complexes ($n = 1-6$). The dissociation energy is defined as follows:

$$\Delta E_e(n) = \{nE[\mathrm{Li}] + (n+1)E[C_6H_6]\} - \{E[\mathrm{Li}_n\cdot(C_6H_6)_{n+1}]\} \qquad n = 1-6 \quad (3)$$

The energy gain $\Delta E_e(n, n-1)$, with the addition of a $Li\cdot C_6H_6$ unit to $Li_{n-1}\cdot(C_6H_6)_n$, is given by

$$\Delta E_e(n, n-1) = \{E[\mathrm{Li}\cdot C_6H_6] + E[\mathrm{Li}_{n-1}\cdot(C_6H_6)]\} - \{E[\mathrm{Li}_n\cdot(C_6H_6)_{n+1}]\} \qquad n = 1-6 \quad (4)$$

TABLE 6: Dissociation Energies (eV) for $Li_n(C_6H_6)_{n+1}$ Complexes ($n = 1-6$)

		$\Delta E_e(n)$		$\Delta E_e(n, n-1)$	
complex	multiplicity[a]	DFT[b]	ReaxFF	DFT[b]	ReaxFF
$Li\cdot(C_6H_6)_2$	2	0.67	0.90	0.52	0.41
$Li_2\cdot(C_6H_6)_3$	3	1.64	2.39	0.82	0.99
$Li_3\cdot(C_6H_6)_4$	4	2.49	3.83	0.69	0.94
$Li_4\cdot(C_6H_6)_5$	5	3.38	5.27	0.74	0.95
$Li_5\cdot(C_6H_6)_6$	6	4.27	7.16	0.74	1.40
$Li_6\cdot(C_6H_6)_7$	7	5.14	8.68	0.72	1.02

[a] The multiplicities are assigned to only DFT calculations. [b] Reference 30.

The quantum calculation data[30] in Table 6 were obtained with the density functional B3LYP/6-31G(d) method, and the geometries of all of the complexes were constrained to the D_{6h} point group for computational efficiency. Moreover, because of the unpaired spin on the lithium atoms, the complexes with multiple lithium atoms can have several different spin states. Vollmer et al.[30] considered the effects and reported that in all the cases the high-spin states were found to be slightly more stable than the corresponding low-spin predictions. Hence, only the DFT data for high-spin states are compared with the ReaxFF data in Table 6. The energies $\Delta E_e(n)$ and $\Delta E_e(n, n-1)$ calculated with the ReaxFF are generally higher than those calculated with DFT. $\Delta E_e(n)$ by DFT converges to about 0.85 eV/Li. However, according to the ReaxFF, $\Delta E_e(n)$ increases from 0.90 (for $Li\cdot(C_6H_6)_2$) to 1.45 eV/Li (for $Li_6\cdot(C_6H_6)_7$) with the size of the complex. From these results, the ReaxFF developed in this study predicts a stronger interaction between a lithium atom and the π electrons of aromatic carbon than the density functional B3LYP/6-31G(d) method does.

3.5.2. Collision Behaviors of a Lithium Atom with a C_{60} Buckyball. Endohedral fullerenes have recently attracted considerable interest. Experimentally, it has been reported that endohedral [Li@C_{60}] and [Na@C_{60}] species are formed during collisions of alkali metal ions with C_{60} vapor molecules, and at least 6 and 20 eV are needed for the insertion of the alkai metal ions to form endoheral $[Li@C_{60}]^+$ and $[Na@C_{60}]^+$, respectively.[31] Tellgmann et al.[32] first produced endohedral [Li@C_{60}] in macroscopic quantities by high-performance liquid chromatography (HPLC) with a Li ion kinetic energy of 30 eV. Ohno et al.[33] investigated the collision behavior between C_{60}^- and alkali metal ions by an ab initio MD simulation at 1000 K and reported that Li@C_{60} can be created when Li^+ with a kinetic energy of ∼5 eV hits the center of a six-membered ring of C_{60}^-, which corresponds well to the experimental result.[31] On the basis of the ab initio MD simulation,[33] we have performed a canonical ensemble MD with the ReaxFF developed in this work. In the present MD simulation, we put one C_{60} molecule and one Li atom in a supercell with given initial velocities. Initially, the Li atom is placed 3 Å from the C_{60}. The Li atom is then set to move toward the C_{60} molecule with a velocity determined by the incident energy. The impinging points are considered in four cases: (i) on a six-membered ring of the C_{60} molecule; (ii) on a five-membered ring; (iii) on a C−C bond; and (iv) on a carbon atom. The simulation temperature is 1000 K, which is the same as that used in the ab initio MD,[33] and the time step is chosen to be 0.25 fs.

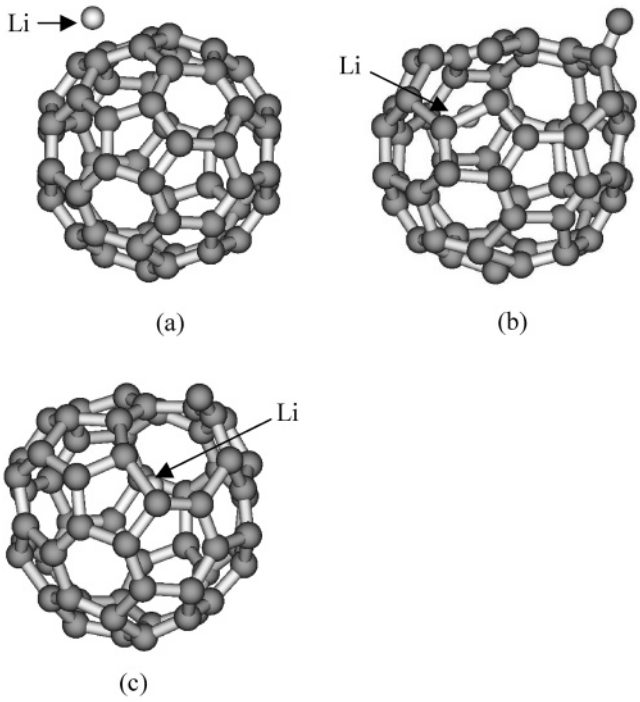

Figure 5. Snapshots of the MD simulation for the formation mechanism of the endohedral [Li@C60] complex where the Li atom hits the center of a six-membered ring of C_{60} with 13 eV of kinetic energy, taken at simulation times of (a) 0 ps, (b) 0.2 fs, and (c) 10 ps. Here, yellow and gray atoms refer to carbon and hydrogen atoms, respectively.

According to the MD simulation with the ReaxFF, the lowest incident energy needed for a Li atom to penetrate a hexagon ring on the C_{60} buckyball and form the endohedral [Li@C_{60}] complex is estimated to be around 13 eV (Figure 5), which is approximately twice as large as the ab initio MD simulation result.[33] The difference in the threshold energy is mainly due to the difference in the radii of Li and Li^+. In the case of the ab initio MD simulation,[33] the interaction between Li^+ and C_{60}^- was investigated while we focused on that between neutral Li and C_{60}. Because the ionic radius of Li^+ is ~0.6−0.9 Å and the hole of a hexagon ring is the same size or slightly smaller,[33] Li^+ can penetrate into the cage through the center of the hexagon ring relatively easily. However, the atomic radius of Li is ~1.5 Å, which is about twice the size of the radius of Li^+. This results in a higher threshold energy for the formation of the endohedral [Li@C_{60}]. As shown in Figure 12, the Li atom in the formed endohedral [Li@C_{60}] complex is at an off-center position in the C_{60} cage, which is in good agreement with previous theoretical works.[34,35] When the incident energy of Li is below 13 eV, the Li atom cannot enter the C_{60} cage and stays outside the center of the hexagon of the cage. Our ReaxFF simulation also indicates that except for a Li atom hitting a six-membered ring of C_{60}, the Li atom cannot be inserted into C_{60} although the incident energy of Li is increased up to 30 eV, similar to the ab initio MD simulation.[33] From these results, we can determine that the endohedral [Li@C_{60}] can be formed by the bombardment of a Li atom with a C_{60}.

4. Summary

We have developed the ReaxFF for Li, Li−H, and Li−C systems. The ReaxFF for Li has been tested against a substantial data set derived from DFT calculations on small clusters and condensed systems covering both reactive and nonreactive aspects of organolithium. Also, the developed ReaxFF is similar or more accurate in expressing organolithium systems than the semiempirical MO methods, PM3 and MNDO. However, the ReaxFF overestimates the van der Waals interaction of Li with benzene rings. Using MD simulations with the ReaxFF, we also found that endohedral [Li@C_{60}] can be formed by the bombardment of a Li atom with a C_{60} if one Li atom with an incident energy of above 13 eV hits a six-membered ring of C_{60} perpendicularly. We believe that this ReaxFF for Li can be used extensively to simulate aspects of organolithium reactivity and interactions between Li and CNT and fullerene.

Acknowledgment. This research was supported by a grant (code no. 04K1501-02210) from the Center for Nanostructured Materials Technology under 21st Century Frontier R&D Programs of the Ministry of Science and Technology, Korea.

Appendix

The ReaxFF parameters for Li optimized in this work are as follows. Here, symbols of the parameters are shown in refs 6 and 7.

TABLE A1: Atom Parameters

			Coulomb parameters			van der Waals parameters			
	r_0 (Å)	$p_{ov/un}$	η (eV)	χ (eV)	γ (Å)	r_{vdW} (Å)	ϵ (kcal/mol)	α	γ_{vdW} (Å)
Li	2.17	−3.08	8.72	1.23	4.42	2.57	0.014	13.62	1.08

TABLE A2: 1−3 Bond Order Correction Parameters

	λ_3	λ_4	λ_5
Li	5.39	0.48	0.05

TABLE A3: Bond Energy and Bond Order Parameters

bond	D^{σ}_e	$p_{be,1}$	$p_{b0,1}$	$p_{b0,2}$
Li−Li	40.7	−0.327	−0.064	4.22
Li−C	57.3	−0.002	−0.009	20.49
Li−H	60.5	−8.065	−0.066	5.01

TABLE A4: van der Waals and Bond Radius Parameters

bond	r^{σ}(Å)	r_{vdW} (Å)	ee (kcal/mol)	aa
Li−C	1.971	1.066	0.292	29.32
Li−H	1.669	1.026	0.406	14.22

References and Notes

(1) *Comprehensive Organometallic Chemistry*; Wilkinson, G., Stone, F. G. A., Abel, E. W., Eds.; Pergamon Press: New York, 1982; Vol. 1.
(2) Setzer, W.; Schleyer, P. v. R. *Adv. Organomet. Chem.* **1985**, *24*, 353.
(3) Mayo, S. L.; Olafson, B. D.; Goddard, W. A. *J. Phys. Chem.* **1990**, *94*, 8897.
(4) Rappé, A. K.; Casewit, C. J.; Colwell, K. S.; Goddard, W. A.; Skiff, W. M. *J. Am. Chem. Soc.* **1992**, *114*, 10024.
(5) Rappé, A. K.; Goddard, W. A. *J. Phys. Chem.* **1991**, *95*, 3358.
(6) van Duin, A. C. T.; Dasgupta, S.; Lorant, F.; Goddard, W. A. *J. Phys. Chem. A* **2001**, *105*, 9396.
(7) van Duin, A. C. T.; Strachan, A.; Stewman, S.; Zhang, Q.; Xu, X.; Goddard, W. A. *J. Phys. Chem. A* **2003**, *107*, 3803.
(8) Zhang, Q.; Çağin, T.; van Duin, A. C. T.; Goddard, W. A.; Qi, Y.; Hector, L. G. *Phys. Rev. B* **2004**, *69*, 045423.
(9) Thiel, W. *QCPE Bull.* **1982**, *2*, 36.
(10) Anders, E.; Koch, R.; Freunscht, P. *J. Comput. Chem.* **1993**, *14*, 1301.
(11) Streitwieser, A.; Williams, J. E.; Alexandratos, S.; McKelvey, J. M. *J. Am. Chem. Soc.* **1976**, *98*, 4778.
(12) Kaufmann, E.; Raghavacharl, K.; Reed, A. E.; Schleyer, P. v. R. *Organometallics* **1988**, *7*, 1597.
(13) Janssens, G. O. A.; Baekelandt, B. G.; Toufar, H.; Martier, W. J.; Schoonheydt, R. A. *J. Phys. Chem.* **1995**, *99*, 3251.
(14) *Jaguar 4.2*; Schrödinger, Inc.: Portland, OR, 1991−2000.
(15) Perdew, J. P.; Burke, K.; Ernserhof, M. *Phys. Rev. Lett.* **1996**, *77*, 3865.

(16) Payne, M. C.; Teter, M. P.; Allan, D. C.; Arias, T. A.; Joannopoulos, J. D. *Rev. Mod. Phys.* **1992**, *64*, 1045.
(17) Monkhorst, H. J.; Pack, J. D. *Phys. Rev. B* **1976**, *13*, 5188.
(18) Fuentealba, P.; Reyes, O. *J. Phys. Chem. A* **1999**, *103*, 1376.
(19) McAdon, M. H.; Goddard, W. A. *J. Phys. Chem*. **1987**, *91*, 2607.
(20) Kittel, C. *Introduction to Solid State Physics*, 7th ed.; John Wiley & Sons: Toronto, 1996; Chapter 3.
(21) Becke, A. D. *J. Chem. Phys.* **1993**, *98*, 5648.
(22) Xu, X.; Goddard, W. A. *Proc. Natl, Acad. Sci. U.S.A.* **2004**, *101*, 2673.
(23) Barbatti, M.; Jalbert, G.; Nascimento, M. A. C. *J. Chem. Phys.* **2001**, *114*, 2213.
(24) Deng, W.-Q.; Xu. X.; Goddard, W. A. *Phys. Rev. Lett.* **2004**, *92*, 166103.
(25) Day, J. P.; Ruoff, A. L. *Phys. Status Solidi A* **1974**, *25*, 205.
(26) Young, D. A.; Ross, M. *Phys. Rev. B* **1984**, *29*, 682.
(27) Boettger, J. C.; Trickey, S. B. *Phys. Rev. B* **1985**, *32*, 3391.
(28) Endo, M.; Kim, C.; Nishimura, K.; Fujino, T.; Miyashita, K. *Carbon* **2000**, *38*, 183.
(29) Suzuki, T.; Hasegawa, T.; Mukai, S. R.; Tamon, H. *Carbon* **2003**, *41*, 1933.
(30) Vollmer, J. M.; Kandalam, A. K.; Curtiss, L. A. *J. Phys. Chem. A* **2002**, *106*, 9533.
(31) Wan, Z.; Christian, J. F.; Anderson, S. L. *Phys. Rev. Lett.* **1992**, *69*, 1352.
(32) Tellgmann, R.; Krawez, N.; Lin, S.-H.; Campbell, E. E. B.; Hertel, I. V. *Nature* **1996**, *382*, 407.
(33) Ohno, K.; Maruyama, Y.; Esfarjani, K.; Kawazoe, Y.; Sato, N.; Hatakeyama, R.; Hirata, T. *Phys. Rev. Lett.* **1996**, *76*, 3590.
(34) Tománek, D.; Li. Y. S. *Chem. Phys. Lett.* **1995**, *243*, 42.
(35) Broclawik, E.; Eilmes, A. *J. Chem. Phys.* **1998**, *108*, 3498.